

## Higher order impact analysis of sandwich panels with functionally graded flexible cores

K. Malekzadeh Fard \*

*Department of Structural Analysis and Simulation, Space Research Institute,  
Malek Ashtar University of Technology, Tehran-Karaj Highway, Post box: 14665-143, Tehran, Iran*

*(Received March 31, 2013, Revised November 01, 2013, Accepted December 15, 2013)*

**Abstract.** This study deals with dynamic model of composite sandwich panels with functionally graded flexible cores under low velocity impacts of multiple large or small masses using a new improved higher order sandwich panel theory (IHSAPT). In-plane stresses were considered for the functionally graded core and face sheets. The formulation was based on the first order shear deformation theory for the composite face sheets and polynomial description of the displacement fields in the core that was based on the second Frostig's model. Fully dynamic effects of the functionally graded core and face-sheets were considered in this study. Impacts were assumed to occur simultaneously and normally over the top and/or bottom of the face-sheets with arbitrary different masses and initial velocities. The contact forces between the panel and impactors were treated as internal forces of the system. Nonlinear contact stiffness was linearized with a newly presented improved analytical method in this paper. The results were validated by comparing the analytical, numerical and experimental results published in the latest literature.

**Keywords:** sandwich panel; FG core; spring-mass system; multi masses; low-velocity impact; contact law

### 1. Introduction

Functionally graded materials (FGM) are the most important materials that are recently used in some practical structures. These materials are used as core of the sandwich panels instead of foam cores. One of the most important problems about sandwich structures is damage caused by low velocity impact. Interfacial shear stresses due to contact forces can be large enough to debond the face sheet from the core. One way for reducing shear stresses is to use functionally graded core; so, the abrupt change in stiffness between the face sheet and core can be eliminated or minimized. The stresses that arise from low velocity impact can be easily understood by analyzing static contact between the impactor and structure (Sun and Sanakar 1985). Many researchers have investigated composite laminates subjected to single mass low velocity impact (Abrate 1998, Choi and Lim 2004, Christoforou and Swanson 1991, Mittal 1987, Sun and Chattopadhyay 1975). Some researchers have studied dynamic response of sandwich structures with flexible cores which are subjected to low velocity impacts (Bernard and Lagace 1989, Malekzadeh *et al.* 2005a, 2007, Mijia and Pizhong 2005). A complete review of the subject of impact on sandwich structures was

---

\*Corresponding author, Associate Professor, E-mail: [k.malekzadeh@gmail.com](mailto:k.malekzadeh@gmail.com)

carried out by Abrate (1998). Apeter *et al.* (2002) studied response of low velocity impact on sandwich beams with functionally graded core using two-dimensional elasticity theory. Various approaches have been proposed for the analysis of impact response of sandwich panels. Classical method decouples local and global responses and ignores any interaction between them. The first order shear deformation theory (FSDT) and higher order shear deformation theory (HSDT) do not consider flexibility of core in transverse direction and the interaction between face-sheets and soft flexible core (Khalili *et al.* 2005, Reddy 1997). Because these theories ignore flexibility of core, researchers have recently used higher order sandwich plate theory (HSAPT) (Frostig 1998, Frostig and Baruch 1994, Sokolinsky *et al.* 2000). Transverse flexibility of the core is taken into account in higher order sandwich plate theory (HSAPT) for a soft core. To express displacement field in the core, Frostig and Thomsen (2004) considered two types of computational models. The first model used vertical shear stresses in the core. The second model assumed a polynomial description of the displacement field in the core. In this case, unknowns were the coefficients of the polynomials in addition to displacements of the face-sheets. In the present formulation, the second Frostig's model was improved and used. Recently, Malekzadeh *et al.* (2005a, b) introduced first order shear deformation theory (FSDT) for face-sheets of sandwich panels with a flexible core. One of the most important parameters in all impact problems is calculating history of impact force. In order to calculate the impact force, many models have been used. For instance, in order to predict impact response of a circular plate, Shivakumar *et al.* (1984) presented a two degree-of-freedom model consisting of four springs for bending, shear and membrane and contact stiffness. They analytically calculated the contact force and contact duration. Other two degree-of-freedom models were proposed by Lal (1983) and Sjoblom *et al.* (1988). Caprino and Teti (1994) used a single degree-of-freedom system to analyze drop weight impact on glass/polyester sandwich panels. Choi and Hong (1994) presented linearized contact law and studied the impact force history on composite laminates. Gong *et al.* (1999) and Gong and Lam (2000) used a spring-mass model with two degrees of freedom in order to determine history of contact force produced during the impact. Anderson (2005) described an investigation of single degree-of-freedom model for large mass impact on composite sandwich laminates. It is common to classify impact as "high velocity" and "low velocity"; but, it was shown by Olsson (2001) that the response type under elastic conditions only depended on the impactor/plate mass ratio. Thus, small mass impact is governed by transient wave propagation and is essentially independent from plate size and boundary conditions. Large mass impact response is essentially quasi-static; i.e., it obeys static load-displacement relations, and strongly depends on plate geometry and boundary conditions. In the past decade, many researchers have used the results of previous works to analysis dynamic response of composite and sandwich structures subjected to large or small mass impacts (Abrate 1998, Gong *et al.* 1999, Anderson and Madenci 2000, Gong and Lam 2000, Hoo Fatt and Park 2001a, b, Olsson 2001, Malekzadeh *et al.* 2005a, 2006). As noted above, much effort has been made to analyze the composite and sandwich structures subjected to low velocity single mass impact using a discrete spring-mass system. As seen, many researchers have focused on sandwich structures subjected to single mass impact while most engineering structures like aerospace structures may be subjected to more than one small mass impactors with different mass velocities, locations and directions. As far as this type of problem is concerned, very limited researches have been done. For the first time, Malekzadeh *et al.* (2006) studied dynamic response of composite sandwich panels with flexible cores under simultaneous low velocity impacts of multiple small masses. The governing equations of motion were derived by higher order sandwich plate theory (HSAPT) and Hamilton's principle. In their research, impacts were assumed to occur normally and

simultaneously over the top face-sheet with similar masses and equal initial velocities of impactors. Also, they improved and used the first Frostig's model in the impact analysis. The contact force between the panel and impactor was treated as internal force of the system. They used linear contact law and Choi's approach (Choi and Hong 1994) in order to obtain a linearized contact law. As no literature could be found on the impact of multiple impactors, Malekzadeh *et al.* (2006) validated their results indirectly by comparing local responses of two cases of double mass and single mass impacts. As seen already, there is no research on dynamic behavior of composite sandwich panels with FG core subjected to arbitrary different impactors with initial velocities, locations and directions. Thus, this study focused on using the newly proposed improved higher order theory to analyze impact on sandwich panels with FG cores. The second Frostig's computational model (Frostig and Thomsen 2004) was improved to express displacement field of the FG core.

In this paper, the second Frostig's model was enhanced by introducing first order shear deformation theory (FSDT) in the face-sheets and incorporating inertia forces and internal in-plane stresses of the functionally graded core to govern equations of motion. The core of sandwich panel was FGM with arbitrary function power law like P-FGM (Bao and Wang 1995), exponential FGM (E-FGM) (Delale and Erdogan 1983), Mori-Tanaka FGM (MT-FGM) (Prakash *et al.* 2008) and sigmoid FGM (S-FGM) (Chung and Chi 2001). The contact forces between the panel and impactors were treated as internal forces of the system. In the case of large mass impacts, in order to calculate histories of the impact forces, an improved two degree-of-freedom spring-mass system was used for each impactor which was solved by the newly improved analytical method. Also, in order to validate the new spring-mass model, especially in an arbitrary location except the center, the sandwich panel with foam core that was subjected to a single large mass impact or multiple large mass impacts was modeled by ABAQUS software.

## 2. Mathematical formulation

In this paper, rectangular composite sandwich panel was considered which was composed of two composite laminated face-sheets and a flexible functionally graded core layer, as shown in Fig. 1. The panel was assumed to have length  $a$ , width  $b$  and total thickness  $h$ , coordinates and sign conventions of which are shown. Below, indices  $t$  and  $b$  refer to top and bottom face-sheets of the panel, respectively. The assumption used in the present analysis was linear elastic small deformation. The sandwich panel was considered to be simply supported and functionally graded core. Effects of secondary contact loadings were assumed to be negligible. Fig. 1 shows that the system consists of  $n$  number of impactor masses striking on the top surface of face-sheet at points with coordinates  $(X_1, Y_1)$ ,  $(X_2, Y_2)$  and  $(X_n, Y_n)$ . Masses and velocities of the impactors were  $(M_1, V_1)$ ,  $(M_2, V_2)$  and  $(M_n, V_n)$ , respectively. Therefore, the contact force only acted over impacted surface of the panel during the first contact duration. Impacts were assumed to occur normally over the top or/and bottom of the face-sheets and it was assumed that vibration of the impactor was negligible.

### 2.1 Governing equations of the system of impactors and panel

The mathematical formulation consisted of derivation of the governing field equations of motion along the appropriate boundary conditions of the face-sheets, core and impactors. They were derived through the Hamilton's principle (Frostig and Thomsen 2004, Malekzadeh *et al.*

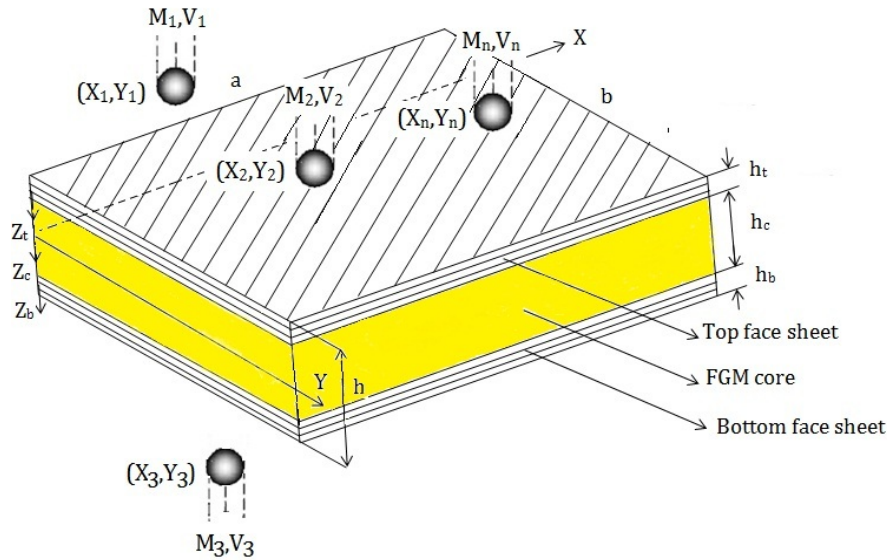


Fig. 1 Sandwich panel with laminated face-sheets, panel coordinates, dimensions and impactors

2005a, b). The formulation was general and for any types of core.

Based on the first order shear deformation theory, displacements  $u$ ,  $v$  and  $w$  of the face sheets along the  $x$ ,  $y$  (longitudinal) and  $z$  (thickness) axes with small linear displacements were expressed through the following relations (Reddy 2003)

$$\begin{aligned}
 u_j(x, z, y, t) &= u_0^j(x, y, t) + z_j \psi_x^j(x, y, t) \\
 v_j(x, z, y, t) &= v_0^j(x, y, t) + z_j \psi_y^j(x, y, t) \\
 w_j(x, z, y, t) &= w_0^j(x, y, t) \quad ; (j = t, b)
 \end{aligned}
 \tag{1}$$

$Z_j$  is vertical coordinate of each face-sheet ( $j = t, b$ ) and is measured downward from the mid-plane of each face-sheet (see Fig. 1). Kinematic equations for the strains in the face sheets were as follows ( $i = t, b$ )

$$\begin{aligned}
 \mathcal{E}_{xx}^i &= u_{0,x}^i + z_i \kappa_{xx}^i ; & \kappa_{xx}^i &= \psi_{x,x}^i \\
 \mathcal{E}_{yy}^i &= v_{0,y}^i + z_i \kappa_{yy}^i ; & \kappa_{yy}^i &= \psi_{y,y}^i \\
 \mathcal{E}_{xy}^i &= u_{0,x}^i + v_{0,y}^i + z_i \kappa_{xy}^i ; & \kappa_{xy}^i &= \psi_{x,y}^i + \psi_{y,x}^i \\
 \mathcal{E}_{xz}^i &= u_{0,z}^i + w_{0,x}^i + z_i \kappa_{xz}^i ; & \kappa_{xz}^i &= \psi_x^i \\
 \mathcal{E}_{yz}^i &= v_{0,z}^i + w_{0,y}^i + z_i \kappa_{yz}^i ; & \kappa_{yz}^i &= \psi_y^i
 \end{aligned}
 \tag{2}$$

The displacement fields for the core were based on the second *Frostig's model* (Frostig and Thomsen 2004)

$$\begin{aligned}
 u_c(x, z, y, t) &= u_0(x, y, t) + z_c u_1(x, y, t) + z_c^2 u_2(x, y, t) + z_c^3 u_3(x, y, t) \\
 v_c(x, z, y, t) &= v_0(x, y, t) + z_c v_1(x, y, t) + z_c^2 v_2(x, y, t) + z_c^3 v_3(x, y, t) \\
 w_c(x, z, y, t) &= w_0(x, y, t) + z_c w_1(x, y, t) + z_c^2 w_2(x, y, t)
 \end{aligned}
 \tag{3}$$

Kinematic relations of the core for a sandwich panel that were based on small deformations were

$$\begin{aligned}
 \epsilon_{xx}^c &= \frac{\partial w_c}{\partial z_c} = (w_1 + 2z_c w_2) \\
 \gamma_{xz}^c &= \frac{\partial u_c}{\partial z_c} + \frac{\partial w_c}{\partial x} = (u_1 + 2z_c w_2 + 3z_c^2 u_3 + w_{0,x} + z_c w_{1,x} + z_c^2 w_{2,x}) \\
 \gamma_{yz}^c &= \frac{\partial v_c}{\partial z_c} + \frac{\partial w_c}{\partial y} = (v_1 + 2z_c v_2 + 3z_c^2 v_3 + w_{0,y} + z_c w_{1,y} + z_c^2 w_{2,y}) \\
 \epsilon_{xx}^c &= \frac{\partial u_c}{\partial x_c} = (u_{0,x} + z_c u_{1,x} + z_c^2 v_{2,x} + z_c^3 v_{3,x}) \\
 \epsilon_{yy}^c &= \frac{\partial v_c}{\partial y_c} = (v_{0,y} + z_c v_{1,y} + z_c^2 v_{2,y} + z_c^3 u_{3,x}) \\
 \gamma_{xy}^c &= \frac{\partial u_c}{\partial y} + \frac{\partial v_c}{\partial x} = (v_{0,x} + z_c v_{1,x} + z_c^2 v_{2,x} + z_c^3 v_{3,x} + u_{0,y} + z_c u_{1,y} + z_c^2 u_{2,y} + z_c^3 w_{3,y})
 \end{aligned}
 \tag{4}$$

Assuming perfect bonding between the core and face-sheets, at the upper and lower face-sheets of core interfaces, the compatibility conditions were

$$\begin{aligned}
 u_c(z = z_c) &= u_0^j + \frac{1}{2}(-1)^k h_j \psi_{xj} \\
 v_c(z = z_{cj}) &= v_0^j + \frac{1}{2}(-1)^k h_j \psi_{xj} \\
 w_c(z = z_{cj}) &= w_0^j
 \end{aligned}
 \tag{5}$$

where  $h_j (j = t, b)$  is thickness of the face sheets where  $k = 1$  when  $j = b$  and  $k = 0$  when  $j = t$ ;  $Z_{ct} = -h_c / 2$  at the top and  $Z_{cb} = h_c / 2$  at the bottom interfaces, respectively (see Fig. 1). Using the displacement fields of the core in Eqs. (3) and (1) and some simplifications, compatibility conditions from Eq. (5) can be written as

$$\begin{aligned}
 u_2 &= (2(u_0^b + u_0^t) - h_b \psi_x^b + h_t \psi_x^t - 4u_0) / h_c^2 \\
 u_3 &= (4(u_0^b - u_0^t) - 2(h_b \psi_x^b + h_t \psi_x^t) - 4h_c u_1) / h_c^3 \\
 v_2 &= (2(v_0^b + v_0^t) - h_b \psi_y^b + h_t \psi_y^t - 4v_0) / h_c^2 \\
 v_3 &= (4(v_0^b - v_0^t) - 2(h_b \psi_y^b + h_t \psi_y^t) - 4h_c v_1) / h_c^3 \\
 w_2 &= 2(w_0^b + w_0^t - 2w_0) / h_c^3 \\
 w_1 &= 2(w_0^b + w_0^t) / h_c
 \end{aligned}
 \tag{6}$$

It can be seen from Eq. (6) that the number of unknowns in the core reduced to three. These unknowns were  $u_0$ ,  $u_1$  and  $w_0$ . The governing equations and boundary conditions were derived

using Hamilton's principle which required that

$$\delta \int_{t_1}^{t_2} (U - T + V) dt = 0 \quad (7)$$

The first variation of the internal potential energy for the sandwich panel could be written as

$$\begin{aligned} \delta U = & \int_{V_t} \left( \sigma_{xx}^t \delta \varepsilon_{xx}^t + \tau_{xz}^t \delta \gamma_{xz}^t + \sigma_{yy}^t \delta \varepsilon_{yy}^t + \tau_{xy}^t \delta \gamma_{xy}^t + \tau_{yz}^t \delta \gamma_{yz}^t \right) dV_t \\ & + \int_{V_b} \left( \sigma_{xx}^b \delta \varepsilon_{xx}^b + \tau_{xz}^b \delta \gamma_{xz}^b + \sigma_{yy}^b \delta \varepsilon_{yy}^b + \tau_{xy}^b \delta \gamma_{xy}^b + \tau_{yz}^b \delta \gamma_{yz}^b \right) dV_b \\ & + \int_{V_c} \left( \sigma_{zz}^c \delta \varepsilon_{zz}^c + \tau_{xz}^c \delta \gamma_{xz}^c + \sigma_{xx}^c \delta \varepsilon_{xx}^c + \sigma_{yy}^c \delta \varepsilon_{yy}^c + \tau_{xy}^c \delta \gamma_{xy}^c + \tau_{yz}^c \delta \gamma_{yz}^c \right) dV_c \end{aligned} \quad (8)$$

The first variation of the kinetic energy, upon assuming homogeneous conditions for the displacement and velocity with respect to the time coordinate is

$$\delta U = \int_{t_1}^{t_2} \left[ \int_0^a \int_0^b \int_{-\frac{h_t}{2}}^{\frac{h_t}{2}} \rho_t (\ddot{u}_{0t} \delta u_{0t} + \ddot{v}_{0t} \delta v_{0t} + \ddot{w}_{0t} \delta w_{0t}) dx dy dz \right. \\ \left. + \int_0^a \int_0^b \int_{-\frac{h_b}{2}}^{\frac{h_b}{2}} \rho_b (\ddot{u}_{0b} \delta u_{0b} + \ddot{v}_{0b} \delta v_{0b} + \ddot{w}_{0b} \delta w_{0b}) dx dy dz \right. \\ \left. + \int_0^a \int_0^b \int_{-\frac{h_c}{2}}^{\frac{h_c}{2}} \rho_c (\ddot{u}_c \delta u_c + \ddot{v}_{0c} \delta v_{0c} + \ddot{w}_c \delta w_c) dx dy dz \right] dt \quad (9)$$

In all cases,  $u$  and  $v$  components are horizontal while  $w$  component is vertical. Also,  $(\ddot{\cdot})$  denotes the second time derivative. Variation of the external work equaled

$$\delta U = - \int_0^a \int_0^b \left( n_{xt} \delta u_{0t} + n_{xb} \delta u_{0b} + n_{yt} \delta v_{0t} + n_{yb} \delta v_{0b} + q_t \delta w_t + q_b \delta w_b \right) dx dy \quad (10)$$

where  $q_t$  and  $q_b$  are the vertical distributed static or dynamic loads exerted on the upper and lower face sheet of plate, respectively;  $n_{xy}$  and  $n_{yj}$  ( $j=t, b$ ) are the in-plane external loads in the longitudinal and transverse direction, respectively, of the upper and the lower face sheets. By Hamilton's principle (Eqs. (9)-(10)) and kinematic relations (Eqs. (1)-(6)), the governing equations of motion could be obtained as follows

$$\begin{aligned} & N_{xx,x}^t + N_{xy,x}^t + \frac{2}{h_c^2} M_{2xx,x}^c + \frac{2}{h_c^2} M_{2xy,y}^c - \frac{4}{h_c^2} M_{Q1xz}^c - \frac{4}{h_c^3} M_{3xx,x}^c - \frac{4}{h_c^2} M_{3xy,y}^c + \frac{12}{h_c^3} M_{Q2xz}^c \\ & = I_0^t u_{0,t}^t + I_1^t \psi_{x,t}^t + u_{0,t} \left( \frac{4}{h_c^3} I_3^c - \frac{2}{h_c^2} I_2^c \right) + u_{1,t} \left( \frac{4}{h_c^3} I_4^c - \frac{2}{h_c^2} I_3^c \right) \\ & + u_{2,t} \left( \frac{4}{h_c^3} I_5^c - \frac{2}{h_c^2} I_4^c \right) + u_{3,t} \left( \frac{4}{h_c^3} I_6^c - \frac{2}{h_c^2} I_5^c \right); \end{aligned} \quad (11)$$

$$\begin{aligned}
 & N_{xx,x}^b + \frac{2}{h_c^2} M_{2xx,x}^c + \frac{2}{h_c^2} M_{2xy,y}^c - \frac{4}{h_c^2} M_{Q1xz}^c + \frac{4}{h_c^3} M_{3xx,x}^c + \frac{4}{h_c^3} M_{3xy,y}^c - \frac{12}{h_c^3} M_{Q2xz}^c \\
 &= I_0^b u_{0,tt}^b + I_1^b \psi_{x,tt}^b - u_{0,tt} \left( \frac{4}{h_c^3} I_3^c + \frac{2}{h_c^2} I_2^c \right) - u_{1,tt} \left( \frac{4}{h_c^3} I_4^c + \frac{2}{h_c^2} I_3^c \right) \\
 & - u_{2,tt} \left( \frac{4}{h_c^3} I_5^c + \frac{2}{h_c^2} I_4^c \right) - u_{3,tt} \left( \frac{4}{h_c^3} I_6^c + \frac{2}{h_c^2} I_5^c \right); \tag{12}
 \end{aligned}$$

$$\begin{aligned}
 & M_{xx,x}^t + M_{xy,y}^t - Q_{xz}^t + \frac{h_t}{h_c^2} M_{2xx,x}^c + \frac{h_t}{h_c^2} M_{2xy,y}^c - \frac{2h_t}{h_c^2} M_{Q1xz}^c \\
 & - \frac{2h_t}{h_c^3} M_{3xx,x}^c - \frac{2h_t}{h_c^3} M_{3xy,y}^c + \frac{6h_t}{h_c^3} M_{Q2xz}^c = I_0^t u_{0,tt}^t + I_2^t \psi_{x,tt}^t \\
 & + u_{0,tt} \left( \frac{2h_t}{h_c^3} I_3^c - \frac{h_t}{h_c^2} I_2^c \right) + u_{1,tt} \left( \frac{2h_t}{h_c^3} I_4^c - \frac{2h_t}{h_c^2} I_3^c \right) \\
 & + u_{2,tt} \left( \frac{2h_t}{h_c^3} I_5^c - \frac{h_t}{h_c^2} I_4^c \right) + u_{3,tt} \left( \frac{2h_t}{h_c^3} I_6^c + \frac{h_t}{h_c^2} I_5^c \right); \tag{13}
 \end{aligned}$$

$$\begin{aligned}
 & M_{xx,x}^b + M_{xy,y}^b - Q_{xz}^b - \frac{h_b}{h_c^2} M_{2xx,x}^c - \frac{h_b}{h_c^2} M_{2xy,y}^c + \frac{2h_b}{h_c^2} M_{Q1xz}^c \\
 & - \frac{2h_b}{h_c^3} M_{3xx,x}^c - \frac{2h_b}{h_c^3} M_{3xy,y}^c + \frac{6h_b}{h_c^3} M_{Q2xz}^c = I_0^b u_{0,tt}^b + I_2^b \psi_{x,tt}^b \\
 & + u_{0,tt} \left( \frac{2h_b}{h_c^3} I_3^c + \frac{h_b}{h_c^2} I_2^c \right) + u_{1,tt} \left( \frac{2h_b}{h_c^3} I_4^c + \frac{2h_b}{h_c^2} I_3^c \right) \\
 & + u_{2,tt} \left( \frac{2h_b}{h_c^3} I_5^c + \frac{h_b}{h_c^2} I_4^c \right) + u_{3,tt} \left( \frac{2h_b}{h_c^3} I_6^c + \frac{h_b}{h_c^2} I_5^c \right); \tag{14}
 \end{aligned}$$

$$\begin{aligned}
 & Q_{xz,x}^t + Q_{yz,y}^t + q_t - \frac{1}{h_c} M_{Q1xz,x}^c - \frac{1}{h_c} M_{Q1yz,y}^c + \frac{1}{h_c} R_z^c + \frac{2}{h_c} M_{Q2xz,x}^c + \frac{2}{h_c} M_{Q2yz,y}^c - \frac{4}{h_c} M_z^c \\
 &= I_0^t w_{0,tt}^t + w_{0,tt} \left( \frac{1}{h_c} I_1^c - \frac{2}{h_c^2} I_2^c \right) + w_{1,tt} \left( \frac{1}{h_c} I_2^c - \frac{2}{h_c^2} I_3^c \right) + w_{2,tt} \left( \frac{1}{h_c} I_3^c - \frac{2}{h_c^2} I_4^c \right); \tag{15}
 \end{aligned}$$

$$\begin{aligned}
 & Q_{xz,x}^b + Q_{yz,y}^b + q_b + \frac{1}{h_c} M_{Q1xz,x}^c + \frac{1}{h_c} M_{Q1yz,y}^c - \frac{1}{h_c} R_z^c + \frac{2}{h_c^2} M_{Q2xz,x}^c + \frac{2}{h_c^2} M_{Q2yz,y}^c - \frac{2}{h_c^2} M_z^c \\
 &= I_0^b w_{0,tt}^b + \frac{1}{h_c} \left( I_1^c w_{0,tt} + I_2^c w_{1,tt} + I_3^c w_{2,tt} \right) - \frac{2}{h_c^2} \left( I_2^c w_{0,tt} + I_3^c w_{1,tt} + I_4^c w_{2,tt} \right); \tag{16}
 \end{aligned}$$

$$\begin{aligned}
& N_{yy,y}^t + N_{xy,x}^t + \bar{n}_{yt} + \frac{2}{h_c^2} M_{2yy,y}^c + \frac{2}{h_c^2} M_{2xy,x}^c - \frac{4}{h_c^2} M_{Q1yz}^c - \frac{4}{h_c^3} M_{3yy,y}^c \\
& - \frac{4}{h_c^3} M_{3xy,y}^c + \frac{12}{h_c^3} M_{Q2yz}^c = I_0^b v_{0,tt}^b + I_1^b \psi_{y,tt}^b + v_{0,tt} \left( \frac{4}{h_c^3} I_3^c - \frac{2}{h_c^2} I_2^c \right) \\
& + v_{1,tt} \left( \frac{4}{h_c^3} I_4^c - \frac{2}{h_c^2} I_3^c \right) + v_{2,tt} \left( \frac{4}{h_c^3} I_5^c - \frac{2}{h_c^2} I_4^c \right) + v_{3,tt} \left( \frac{4}{h_c^3} I_6^c - \frac{2}{h_c^2} I_5^c \right);
\end{aligned} \tag{17}$$

$$\begin{aligned}
& M_{yy,y}^t + M_{xy,y}^t - Q_{xz}^t + \frac{h_t}{h_c^2} M_{2yy,y}^c + \frac{h_t}{h_c^2} M_{2xy,y}^c - \frac{2h_t}{h_c^2} M_{Q1yz}^c \\
& - \frac{2h_t}{h_c^3} M_{3yy,y}^c - \frac{2h_t}{h_c^3} M_{3xy,y}^c + \frac{6h_t}{h_c^3} M_{Q2xz}^c = I_1^t v_{0,tt}^t + I_2^t v_{0,tt}^t \\
& + v_{0,tt} \left( \frac{2h_t}{h_c^3} I_3^c - \frac{h_t}{h_c^2} I_2^c \right) + v_{1,tt} \left( \frac{2h_t}{h_c^3} I_4^c - \frac{2h_t}{h_c^2} I_3^c \right) \\
& + v_{2,tt} \left( \frac{2h_t}{h_c^3} I_5^c - \frac{h_t}{h_c^2} I_4^c \right) + v_{3,tt} \left( \frac{2h_t}{h_c^3} I_6^c - \frac{h_t}{h_c^2} I_5^c \right);
\end{aligned} \tag{18}$$

$$\begin{aligned}
& M_{yy,y}^b + M_{xy,y}^b - Q_{xz}^b - \frac{h_b}{h_c^2} M_{2yy,y}^c - \frac{h_b}{h_c^2} M_{2xy,y}^c + \frac{2h_b}{h_c^2} M_{Q1xz}^c \\
& - \frac{2h_b}{h_c^3} M_{3yy,y}^c - \frac{2h_b}{h_c^3} M_{3xy,y}^c + \frac{6h_b}{h_c^3} M_{Q2yz}^c = I_1^b v_{0,tt}^b + I_2^b \psi_{y,tt}^b \\
& + v_{0,tt} \left( \frac{2h_b}{h_c^3} I_3^c + \frac{h_b}{h_c^2} I_2^c \right) + v_{1,tt} \left( \frac{2h_b}{h_c^3} I_4^c + \frac{h_b}{h_c^2} I_3^c \right) \\
& + v_{2,tt} \left( \frac{2h_b}{h_c^3} I_5^c + \frac{h_b}{h_c^2} I_4^c \right) + v_{3,tt} \left( \frac{2h_b}{h_c^3} I_6^c + \frac{h_b}{h_c^2} I_5^c \right);
\end{aligned} \tag{19}$$

$$\begin{aligned}
& Q_{xz,y}^c + Q_{xz,y}^c + \frac{4}{h_c^2} M_{Q2yz,x}^c + \frac{4}{h_c^2} M_{Q2xz,x}^c - \frac{8}{h_c^2} M_z^c \\
& = w_{0,tt} \left( I_1^c + \frac{4}{h_c^2} I_2^c \right) + w_{1,tt} \left( I_1^c + \frac{4}{h_c^2} I_3^c \right) + w_{2,tt} \left( I_2^c + \frac{4}{h_c^2} I_4^c \right);
\end{aligned} \tag{20}$$

$$\begin{aligned}
& M_{xx,x}^c + M_{xy,y}^c - Q_{xz}^c - \frac{4}{h_c^2} M_{3xx,x}^c - \frac{4}{h_c^2} M_{3xy,y}^c + \frac{12}{h_c^2} M_{Q2xz}^c \\
& = u_{0,tt} \left( I_1^c + \frac{4}{h_c^2} I_3^c \right) + u_{1,tt} \left( I_2^c + \frac{4}{h_c^2} I_4^c \right) + u_{2,tt} \left( I_3^c + \frac{4}{h_c^2} I_5^c \right) + u_{3,tt} \left( I_4^c + \frac{4}{h_c^2} I_6^c \right);
\end{aligned} \tag{21}$$

$$\begin{aligned}
 &M_{yy,y}^c + M_{xy,y}^c - Q_{xz}^c - \frac{4}{h_c^2} M_{3yy,y}^c - \frac{4}{h_c^2} M_{3xy,y}^c + \frac{12}{h_c^2} M_{Q2,xz}^c \\
 &= v_{0,t} \left( I_1^c + \frac{4}{h_c^2} I_3^c \right) + v_{1,t} \left( I_2^c + \frac{4}{h_c^2} I_4^c \right) + v_{2,t} \left( I_3^c + \frac{4}{h_c^2} I_5^c \right) + v_{3,t} \left( I_4^c + \frac{4}{h_c^2} I_6^c \right);
 \end{aligned} \tag{22}$$

$$\begin{aligned}
 &N_{xx,x}^t + N_{xy,x}^t - \frac{4}{h_c^2} M_{2xx,x}^c - \frac{4}{h_c^2} M_{2xy,y}^c + \frac{8}{h_c^2} M_{Q1,xz}^c \\
 &= u_{0,t} \left( I_0^c + \frac{4}{h_c^2} I_2^c \right) + u_{1,t} \left( I_1^c + \frac{4}{h_c^2} I_3^c \right) + u_{2,t} \left( I_2^c + \frac{4}{h_c^2} I_4^c \right) + u_{3,t} \left( I_3^c + \frac{4}{h_c^2} I_5^c \right);
 \end{aligned} \tag{23}$$

$$\begin{aligned}
 &N_{yy,x}^t + N_{xy,x}^t - \frac{4}{h_c^2} M_{2yy,y}^c - \frac{4}{h_c^2} M_{2xy,y}^c + \frac{8}{h_c^2} M_{Q1,yz}^c \\
 &= v_{0,t} \left( I_0^c + \frac{4}{h_c^2} I_2^c \right) + v_{1,t} \left( I_1^c + \frac{4}{h_c^2} I_3^c \right) + v_{2,t} \left( I_2^c + \frac{4}{h_c^2} I_4^c \right) + v_{3,t} \left( I_3^c + \frac{4}{h_c^2} I_5^c \right);
 \end{aligned} \tag{24}$$

where

$$\begin{aligned}
 \{N_{xx}^i, M_{xx}^i\} &= \int_{-\frac{h_i}{2}}^{\frac{h_i}{2}} (1, z_i) \sigma_{xx}^i dz_i, \quad \{N_{yy}^i, M_{yy}^i\} = \int_{-\frac{h_i}{2}}^{\frac{h_i}{2}} (1, z_i) \sigma_{yy}^i dz_i, \quad \{N_{yy}^i, M_{yy}^i\} = \int_{-\frac{h_i}{2}}^{\frac{h_i}{2}} (1, z_i) \sigma_{yy}^i dz_i \\
 \{Q_{xz}^i\} &= \int_{-\frac{h_i}{2}}^{\frac{h_i}{2}} \tau_{xz}^i dz_i, \quad \{Q_{yz}^i\} = \int_{-\frac{h_i}{2}}^{\frac{h_i}{2}} \tau_{yz}^i dz_i, \quad i = t, b \\
 \{N_{xx}^c, M_{nxx}^c\} &= \int_{-\frac{h_c}{2}}^{\frac{h_c}{2}} (1, z_c^n) \sigma_{xx}^c dz_c, \quad \{N_{yy}^c, M_{myy}^c\} = \int_{-\frac{h_c}{2}}^{\frac{h_c}{2}} (1, z_c^n) \sigma_{yy}^c dz_c, \\
 \{N_{xy}^c, M_{nxy}^c\} &= \int_{-\frac{h_c}{2}}^{\frac{h_c}{2}} (1, z_c^n) \tau_{xy}^c dz_c, \quad \{Q_{xz}^c, M_{Qnxx}^c\} = \int_{-\frac{h_c}{2}}^{\frac{h_c}{2}} (1, z_c^n) \tau_{xz}^c dz_c, \\
 \{Q_{yz}^c, M_{Qnyz}^c\} &= \int_{-\frac{h_c}{2}}^{\frac{h_c}{2}} (1, z_c^n) \tau_{xz}^c dz_c, \quad \{R_z^c, M_z^c\} = \int_{-\frac{h_c}{2}}^{\frac{h_c}{2}} (1, z_c) \sigma_{zz}^c dz_c
 \end{aligned} \tag{25}$$

In Eqs. (11)-(24),  $I_n^i$  ( $n = 0, 1, 2$ ), ( $i = t, b, c$ ) are moments of inertia for the upper face-sheet, lower face-sheet and core, respectively, as follows

$$I_n^i = \int_{-\frac{h_i}{2}}^{\frac{h_i}{2}} z_i^n \rho_i dz_i \quad (i = t, b, c) \tag{26}$$

### 2.2 Impact force calculation

In equations of motion obtained for the panel and impactors,  $q_j$  ( $j = t, b$ ) are impact forces described by series expansion as follows

$$q_j(x, y, t) = \sum_{m=1}^{\infty} \sum_{n=1}^{\infty} \left[ \sum_{i=1}^N q_{mi}^t(t) \right] \sin(\alpha_m x) \sin(\beta_n y) \tag{27}$$

where  $\alpha_m, \beta_n = m\pi x/a, n\pi y/b$  and  $q_{mn}^i$ , ( $i = 1, 2, \dots, N$ ) are Fourier coefficients. The concentrated contact loads  $F_c^i(t)$  located at points  $(x_i, y_i)$  of the upper face-sheets became

$$q_{mn}^i(t) = \frac{4F_c^i(t)}{ab} \sin(\alpha_m x_i) \sin(\beta_n y_i) \quad (28)$$

$F_c^i(t)$  are impact forces that must be calculated.

### Large mass impact

In order to calculate the impact force at any impact point  $(x_i, y_i)$ , two degree-of-freedom spring-mass model was considered for mathematical modeling of the impact phenomena. Then, it was linearized by the newly presented improved analytical method in this paper. In this model, impactors and target structure were shown by masses  $M_I^i$  and  $M_{eff}^i$ , respectively. Indentation of impactors in the target structure were shown by spring with stiffness  $K_c^i$  ( $i = 1, 2, \dots, N$ ) and transverse local stiffness of impacted structure at points  $(x_i, y_i)$ , ( $i = 1, 2, \dots, N$ ) were shown by spring with stiffness of  $K_g^i$  (Fig. 2). In Fig. 2,  $K_g^i$  is equal to local stiffness of the panel in  $i^{\text{th}}$  impactor point and for any impactor, it was defined as

$$q_{mn}^i(t) = \frac{4F_c^i(t)}{ab} \sin(\alpha_m x_i) \sin(\beta_n y_i) \quad (29)$$

Because the impactors influenced different points, Eq. (29) was capable of statically calculating stiffness of the structure at any point. Effective mass of the simply supported sandwich panel was obtained as follows (Khalili *et al.* 2007)

$$\begin{cases} M_{eff}^p = \frac{1}{4} M_{tot}, & M_t = ab \int_{-\frac{h}{2}}^{\frac{h}{2}} \rho_i(z) dz_i, & i = t, b, c \\ M_{tot} = M_t + M_c + M_b \end{cases} \quad (30)$$

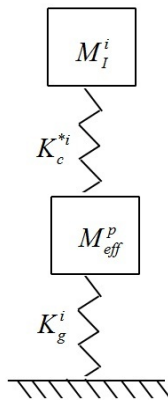


Fig. 2 Linearized spring-mass for the  $i^{\text{th}}$  impactor

The contact deformation between target structure and  $i^{\text{th}}$  impactor was defined as

$$\delta^i(t) = Z_1^i(t) - Z_2^i(t) \tag{31}$$

Using the Hertz's contact law, impact force could be written as (Yang and Sun 1981)

$$F^i(t) = K_c^i \delta_i^n \tag{32}$$

where  $n$  is 1.5 for all of the impactors (Willis 1966).  $K_c^i$  ( $i = 1, 2, \dots, N$ ) is introduced as follows

$$K_c^i = \frac{4}{3} \frac{\text{sqr}t(R^i)}{\pi(K_1^i + K_2^i)} \tag{33}$$

$K_1^i$  and  $K_2^i$  are defined as (Yang and Sun 1981)

$$K_k^i = \frac{1 - (v_k^i)^2}{\pi E_k^i}, \quad k = 1, 2 \tag{34}$$

In the present model, linear form of modified Hertzian law was used. Therefore, to obtain the linearized contact deformation; i.e., the contact force between the  $i^{\text{th}}$  impactor and  $i^{\text{th}}$  impacted point, the linearized contact stiffness  $K_c^*$  was used as follows

$$F_c^i = K_c^{*i} [Z_2^i(t) - Z_1^i(t)] \tag{35}$$

Using the governing equations of motion for two degree-of-freedom spring-mass system (Fig. 2), Choi's linearized Eq. (35) (Choi and Lim 2004) and also some simplifications, the impact force can be obtained as follows

$$F_c^i(t) = \frac{K_c^{i*} V^i}{(\phi_2^i - \phi_1^i)} \left[ \frac{1 - \phi_2^i}{\omega_2^i} \sin(\omega_2^i t) - \frac{1 - \phi_1^i}{\omega_1^i} \sin(\omega_1^i t) \right] \tag{36}$$

where

$$\begin{aligned} \omega_1^i &= \frac{1}{2} \left( \frac{(N^i+1)K_c^{i*} + K_g^i}{N^i M_I^i} - \sqrt{\left( \frac{(N^i+1)K_c^{i*} + K_g^i}{N^i M_I^i} \right)^2 - 4 \frac{K_c^{i*} K_g^i}{N^i M_I^i}} \right) \\ \omega_2^i &= \frac{1}{2} \left( \frac{(N^i+1)K_c^{i*} + K_g^i}{N^i M_I^i} + \sqrt{\left( \frac{(N^i+1)K_c^{i*} + K_g^i}{N^i M_I^i} \right)^2 - 4 \frac{K_c^{i*} K_g^i}{N^i M_I^i}} \right) \\ \left( \frac{B^i}{A^i} \right)_{\omega_1^i} &= \frac{K_c^{i*}}{K_c^{i*} - M_I^i \omega_1^{i2}} = \phi_1^i, \quad \left( \frac{B^i}{A^i} \right)_{\omega_2^i} = \frac{K_c^{i*}}{K_c^{i*} - M_I^i \omega_2^{i2}} = \phi_2^i \end{aligned} \tag{37}$$

where  $N^i = M_{eff}^i / M_I^i$ . In Eq.(36),  $K_c^{i*}$  ( $i = 1, 2, \dots, N$ ) are unknowns and must be found. To obtain them, first, Taylor's binomial expansion of trigonometric sin and cosine functions were used as

follows.

$$\begin{aligned} \sin(\omega_1^i t) &= (\omega_1^i t) - \frac{1}{6}(\omega_1^i t)^3 \\ \sin(\omega_2^i t) &= (\omega_2^i t) - \frac{1}{6}(\omega_2^i t)^3 \end{aligned} \tag{38}$$

By substituting Eq. (37) in Eq. (36), taking the first time derivative of Eq. (37) and some simplification, maximum contact time and corresponding maximum contact force can be written as follows

$$t_{\max}^i = \sqrt{\frac{2N^i M_I^i}{(N^i + 1)K_c^*}} \tag{39}$$

$$F_{c\max}^i = \frac{2}{3}V^i \sqrt{\frac{2N^i M_I^i K_c^*}{(N^i + 1)}} \tag{40}$$

By considering Eq. (38) and Choi's linearized stiffness equation,  $K_c^* = K_c^{1/n} F_{\max}^{n-1/n}$  (Choi and Lim 2004), an analytical equation of linearized contact stiffness could be obtained as follows

$$K_c^{i*} = \left(\frac{2\sqrt{2}}{3}\right)^{\frac{2(n-1)}{n+1}} \left(\frac{N^i}{N^i + 1}\right)^{\frac{n-1}{n+1}} (V^i)^{\frac{2(n-1)}{n+1}} (K_c^i)^{\frac{2(n-1)}{n+1}} (M_I^i)^{\frac{n-1}{n+1}} \tag{41}$$

By substituting Eq. (41) in Eq. (36), the impact force function can be easily calculated. The impact solution for a rectangular plate with simply supported boundary conditions at the top and bottom face-sheets was assumed to be in the following form in Eq. (42):

In Eq. (42),  $C_{u_0^i}^{mn}$ ,  $C_{v_0^i}^{mn}$ ,  $C_{w_0^i}^{mn}$ ,  $C_{\psi_x^i}^{mn}$ ,  $C_{\psi_y^i}^{mn}$ ,  $C_{u_k^i}^{mn}$ ,  $C_{v_k^i}^{mn}$  and  $C_{w_l^i}^{mn}$  are Fourier coefficients that are time-dependent unknowns and m and n are half wave numbers along x and y directions, respectively.  $j = t, b$ , where t and b mean the top and bottom face-sheets, respectively.

$$\begin{bmatrix} u_0^j(x, y, t) \\ v_0^j(x, y, t) \\ w_0^j(x, y, t) \\ \psi_x^j(x, y, t) \\ \psi_y^j(x, y, t) \\ u_k^j(x, y, t) \\ v_k^j(x, y, t) \\ w_l^j(x, y, t) \end{bmatrix} = \sum_{n=1}^{\infty} \sum_{m=1}^{\infty} \begin{bmatrix} C_{u_0^i}^{mn}(t) \cos(\alpha_m x) \sin(\beta_n y) \\ C_{v_0^i}^{mn}(t) \sin(\alpha_m x) \cos(\beta_n y) \\ C_{w_0^i}^{mn}(t) \sin(\alpha_m x) \sin(\beta_n y) \\ C_{\psi_x^i}^{mn}(t) \cos(\alpha_m x) \sin(\beta_n y) \\ C_{\psi_y^i}^{mn}(t) \sin(\alpha_m x) \cos(\beta_n y) \\ C_{u_k^i}^{mn}(t) \cos(\alpha_m x) \sin(\beta_n y) \\ C_{v_k^i}^{mn}(t) \sin(\alpha_m x) \cos(\beta_n y) \\ C_{w_l^i}^{mn}(t) \sin(\alpha_m x) \sin(\beta_n y) \end{bmatrix}, \quad (k = 0, 1, 2, 3), (l = 0, 1, 2) \tag{42}$$

Using Eqs. (27)-(42), the solution was determined by substituting Eq. (42) in the governing Eqs. (11)-(25), which yielded a set of coupled ordinary differential equations, instead of the set of

partial differential equations

$$[M]\{\ddot{c}\} + [M]\{c\} = \{Q\} \tag{43}$$

Therefore, the problem of impact on a sandwich panel was reduced to the standard structural response equations.  $[K]$  is  $(15 \times m \times n) \times (15 \times m \times n)$  stiffness matrix,  $[M]$  is  $(15 \times m \times n) \times (15 \times m \times n)$  square mass matrix and  $[Q]$  is  $(15 \times m \times n) \times (1)$  vector of impact forces. By this method, the governing equations of motion of the impactors were not coupled with the motion equations of the system. Therefore, the set of second order differential equations could be easily solved using Runge-Kutta numerical method and MATLAB tools.

Small mass impact

Wave controlled (small mass) impact response occurs when the impactor mass is smaller than one fifth of the wave affected plate mass when a major wave first reaches a boundary (Olsson 2000). The contact force between the  $i^{\text{th}}$  impactor and the impacted face-sheet of the sandwich panel during the impact can usually be approximated and governed by the nonlinear Hertzian contact law using Eq. (32) (Gong and Lam 2000). The equation of motion for the  $i^{\text{th}}$  impactor can be written as

$$M_I^i \ddot{w}_p^i + F^i(t) = 0, \quad w_p^i(t=0) = 0, \quad \dot{w}_p^i(t=0) = V^i \tag{44}$$

Where  $M_I^i$  is mass of the  $i^{\text{th}}$  impactor,  $w_p^i$  is displacement of the vimpactor and  $F^i(t)$  is the contact force between the  $i^{\text{th}}$  impactor and sandwich panel (See Eq. (32)).  $i$  is a superscript and denotes the vimpact ( $i = 1, 2, \dots, N$ ). As Eq. (32) can be highly nonlinear, seeking an analytic solution for the contact force might pose a formidable task. The approach by Choi (Choi and Lim 2004) employed a linearized effective contact law for the  $i^{\text{th}}$  impactor-panel contact and the assumption of an approximate linear relationship between the equivalent contact force and contact deformation (See Eq. (35)). Similar to Eq. (43), dynamic equations of motion of the system of panel and impactors in terms of deformation and rotation components in the face-sheets and core were derived using the field equations along with the constitutive relations and governing equations. Then, by applying the Galerkin method, the governing equations were reduced to the following system of coupled ordinary differential equations (Malekzadeh *et al.* 2006)

$$M_I^i \ddot{w}_p^i + F^i(t) = 0, \quad w_p^i(t=0) = 0, \quad \dot{w}_p^i(t=0) = V^i \tag{45}$$

$$[M]\{\ddot{c}\} + [M]\{c\} = \{Q\} \quad c(t=0) = [0]$$

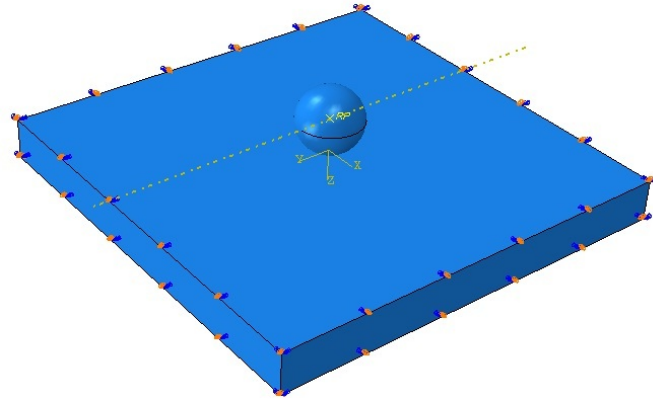
Where  $F^i(t) = K_c^* \alpha^i$  and  $\alpha^i = w_p^i - w_{0r}(x_i, y_i)$  are related to transverse displacements of the impactors  $w_p^i$  and the panel  $w_{0r}(x_i, y_i)$  in the impact locations, respectively.  $i$  is a superscript and denotes the  $i^{\text{th}}$  impact ( $i = 1, 2, \dots, N$ ).

Therefore, the problem of small mass impact on a sandwich panel was reduced to the standard structural response equation (coupled complete solution).  $[M]$  is  $(10 \text{ mn}) \times (10 \text{ mn})$  square mass matrix,  $[K]$  is  $(10 \text{ mn}) \times (10 \text{ mn})$  square symmetric stiffness matrix and  $\{Q\}$  is  $(10 \text{ mn}) \times 1$  vector of impact forces. The system of coupled Eq. (45) had  $10 \text{ mn} \times N$  coupled ordinary differential equations and could be readily solved using a suitable numerical integration procedure.

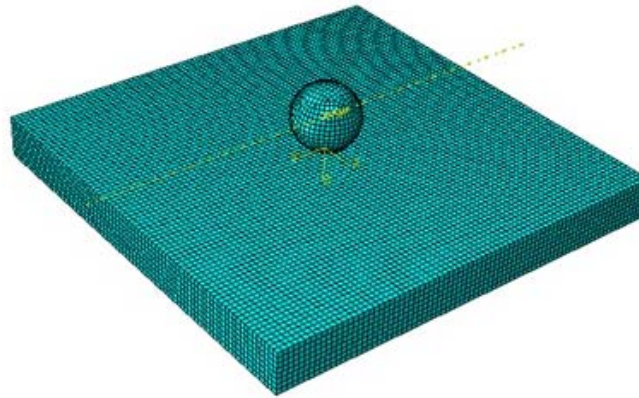
These non-linear second order differential equations can be solved by the Runge-Kutta numerical method by ODE tools of MATLAB-7.0 software.

### 3. Numerical results and discussion

The present two degree-of-freedom (TDOF) spring-mass model yielded the analytic functions which described history of contact force as well as deflections of the large mass impactor and panel at the impact point (See Eqs. (29-36)). In the case of small mass impact, the coupled nonlinear differential Eq. (45) had to be solved (complete solution). In order to verify and validate the results, at first, an example was considered. For single large mass impact, the numerical and finite element results from the present study were compared with the experimental and theoretical results in the literature (Anderson 2005, Malekzadeh *et al.* 2006). The sandwich panel considered for validation included two composite face-sheets and a flexible foam core. Geometrical and mechanical properties of the panel used for the large mass impact are shown in Table 1. The layup of this panel is  $[0_2, 90_2, 0_2 / \text{core} / 0_2, 90_2, 0_2]$ . In this paper, to investigate the impact problem, in addition to the presented method, a finite element procedure was considered. Therefore, for simulating the impact phenomena, ABAQUS software (version 6.8-1) was used. Numerical analysis is often performed by the finite element solver ABAQUS/Explicit, which uses a central difference rule to integrate the equations of motion explicitly (Dassault System's Simulia Corp. 2008). In this study, sandwich panel with foam core and impactor was meshed using SC8R elements, as shown in Figs. 3(a) and (b). In order to model the impactor, it was assumed to behave as a rigid body and no property was assigned, which meant that the impactor had infinite rigidity. This assumption has been used by many researchers (Kistler and Waas 1999, Tarfaoui *et al.* 2008). In order to model the impact problem by FE methods, it is clear that a contact constraint should be used between the target structure and impactor. For contact modeling, there are many contact laws that can be applied in ABAQUS. In this paper, the clearance between two surfaces (top face-sheet and surface of impactor) was considered to be zero and Hertzian contact law was used between the sandwich panel and impactor. The core was flexible; therefore, simply support boundary conditions were applied to the top and bottom face-sheets (Fig. 3(a)). In addition, in order to define the boundary conditions for the impactor, movement of the impactor in all directions was restricted, except for the translation along to the normal vector of the sandwich panel. Initial velocity of the impactor was specified as the predefined field available in ABAQUS FE code at the reference point of the rigid impactor. Furthermore, in the case of rigid impactor, since no material properties were assigned, mass of the impactor should be assigned at the reference point of the impactor (Fig. 3(a)). This method applies boundary conditions for the impactor and the same target structures have been used in previous works (Khalili *et al.* 2011, Swanson *et al.* 1991). In Fig. 4, the predicted and experimental contact force histories of the panel are shown. The contact force histories were also compared with the predictions in references (Anderson 2005, Malekzadeh *et al.* 2006). It can be seen in Fig. 4 that histories of contact forces for both two-degree-of-freedom (TDOF) spring-mass (See Eq. (36)) and FE models were in good agreement with the previous works in the literature. Therefore, the TDOF model could be easily applied in large mass impact problems. As mentioned in the introduction, there is only one research on the dynamic behavior of composite sandwich panels with foam core subjected to two impactors, which was published in 2006 by Malekzadeh *et al.* (2006). Therefore, the current small mass multi impacts results can be validated by this reference. Geometrical and mechanical properties of the panel used for impact analysis are shown in Table 1. Layup of the panel is  $[0_2, 90_2, 0_2 / \text{core} / 0_2, 90_2, 0_2]$ . The boundary conditions of the top face-sheet and bottom face-sheet were simply supported. In this example, mass of the impactors was 5 g or 10 g while impact velocity of all impactors was 3 m/s. Tips of the impacting masses were identical to diameter of 10 mm. The impactors were impacted on the top



(a) Boundary conditions of the top and bottom face-sheets and impactor



(b) mesh used in FE modeling of the impactor and the composite sandwich panel

Fig. 3 FE model of the composite sandwich panel and impactor

Table 1 Material properties of the sandwich panel and impactor

Properties	Sandwich panel with foam core		Impactor	
	Face sheets (LTM45EL-CF0111 Carbon)	core (110WF xolymethacryimide foam)	Properties	
$E_{11}$ (GPa)	54	0.18	$E$ (GPa)	207
$E_{22}$ (GPa)	54	0.18	$\nu$	0.3
$E_{33}$ (GPa)	4.84	0.18	Radius (mm)	12.7
$G_{12}$ (GPa)	3.16	0.07	Velocity (m/s)	3
$G_{13} = G_{23}$ (GPa)	1.87	0.07	Mass (kg)	1.8
$\nu_{12}$ (GPa)	0.06	0.286		
$\nu_{13} = \nu_{23}$ (GPa)	0.313	0.286		
$\rho$ (kg/m <sup>3</sup> )	1511	110		
$h_c$ (mm)	–	12.7		
$a = b$ (mm)	158.7	158.7		

face-sheet in locations  $(x_1 = a/6, y_1 = b/2)$  and  $(x_2 = 5a/6, y_2 = b/2)$ . The predicted maximum indentations from the present formulations (Eq. (45)) are presented in Fig. 5, which was compared with results by Malekzadeh (Malekzadeh *et al.* 2006). It can be seen that these results (based on *the second Frostig's model and coupled complete solution*) were in quite good agreement with Malekzadeh's model (based on *the first Frostig's model and coupled complete solution*). For more validation of the newly presented method, the sandwich panel with given properties in Table 1 subjected to two impactors was modeled in ABAQUS software. Then, the obtained results by the present complete solution were validated. Mass of the small impactors was 10 g while the impact velocity of all impactors was 4 m/s. Tips of the impacting masses were identical to diameter of 20 mm. The impactors were impacted on the top face-sheet in locations  $(x_2 = a/4, y_2 = b/2)$  and  $(x_2 = a/2, y_2 = b/2)$ . Deflections of the top face-sheet obtained from the presented method and FE methods are presented in Fig. 6. Maximum discrepancy between the results was 5.31%.

### 3.1 Dynamic response of a sandwich panel with FGM core subjected to multiple small mass impactors with equal masses and the same directions

In this section, dynamic response of a sandwich panel with FG core subjected to multiple small mass impactors is studied. In Table 2, material properties of the face-sheets and core and geometrical properties of the sandwich panels which were used for the small mass impact analysis are shown. Indexes 1 and 2 for the FG core properties are given in Table 2, representing the properties of the lowest ( $z_c = h_c/2$ ) and top surfaces ( $z_c = -h_c/2$ ) of the FG core, respectively. Core of the sandwich panel was functionally graded material with arbitrary FG materials; but, in this section, it was assumed to be power-law function (P-FGM) with power  $P = 1$ . Geometrical properties of the panel were  $a = 158$  mm,  $a/b = 1$ ,  $a/h = 3.16$  and  $h_c/h = 0.88$ . At first, dynamic response of a sandwich panel with the properties given in Table 2 subjected to two impactors with equal initial velocities and small masses was studied.

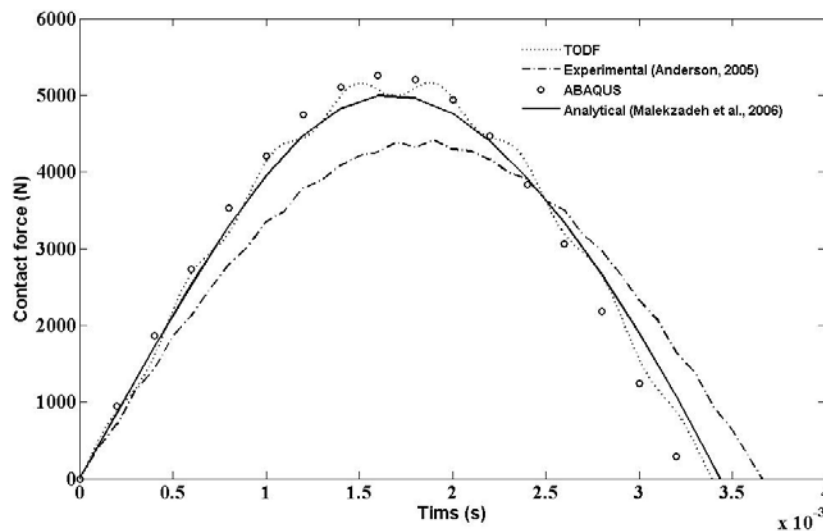


Fig. 4 The predicted impact force histories at the center of the panel

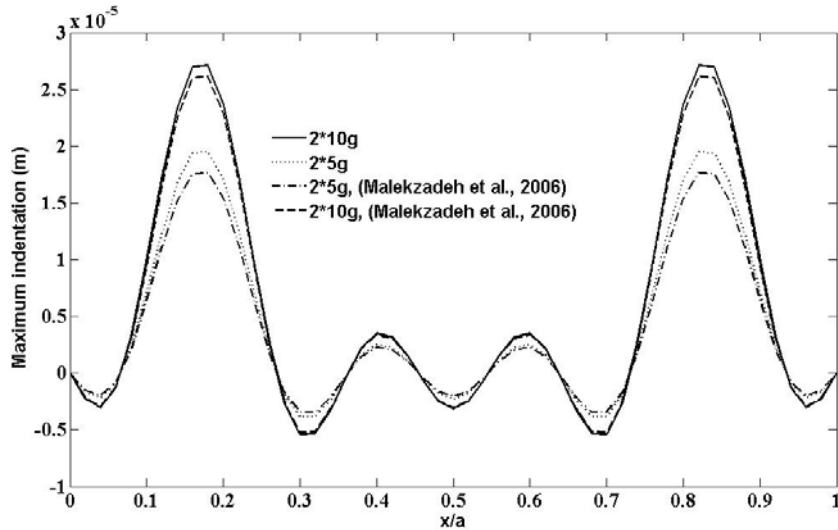


Fig. 5 Predicted maximum indentations along the section  $y = b/2$

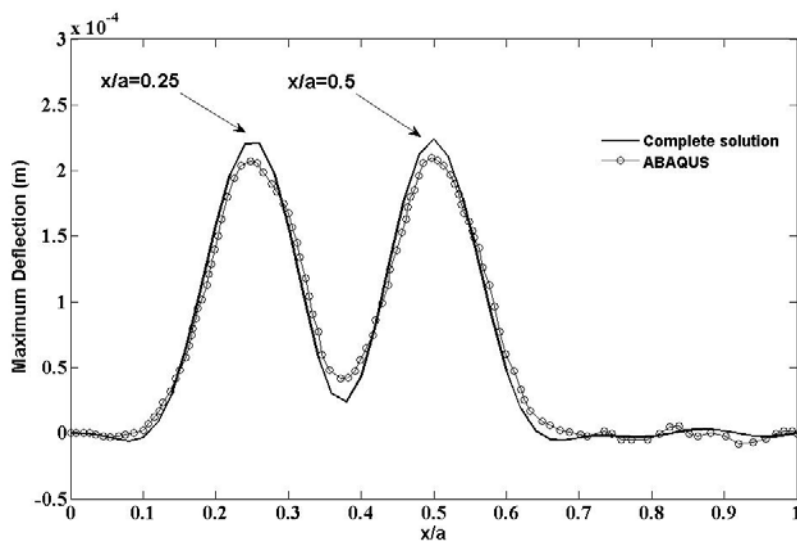


Fig. 6 Predicted maximum deflection of the top face-sheet along the section  $y = b/2$

As no literature could be found on the impact of multiple impactors on sandwich panels with functionally graded core, the present formulation was indirectly validated by comparing local responses of two cases of double small masses and a single small mass impacts at contact points with identical locations satisfying Eq. (35) of Ref. (Malekzadeh *et al.* (2006)). In this example, mass of impactors was 10 g with radius of 10 mm and the panel was simultaneously impacted in two locations ( $x_1 = a/6, y_1 = b/2$ ) and ( $x_2 = 5a/6, y_2 = b/2$ ). In this example, the impact velocity of

all impactors was 3 m/s. The two cases were solved using both spring mass and coupled complete models (see Eqs. (36) and (45)) and their local dynamic characteristics in location ( $x_1 = a/6, y_1 = b/2$ ) were compared. With these definitions, the left half of these two systems was identical. The two cases were solved and their local dynamic characteristics in location ( $x_1 = a/6, y_1 = b/2$ ) were compared. It is clear that the dynamic behavior of the panel in both cases should be

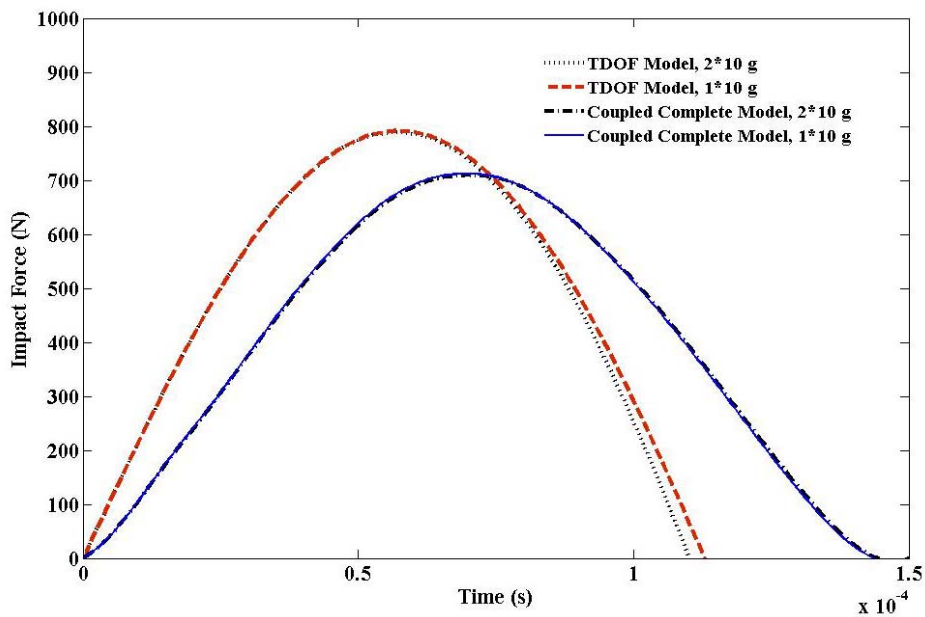


Fig. 7 Comparing the contact force histories of two cases over the top face-sheet of the panel with FGM core in the identical contact location ( $x_1 = a/6, y_1 = b/2$ )

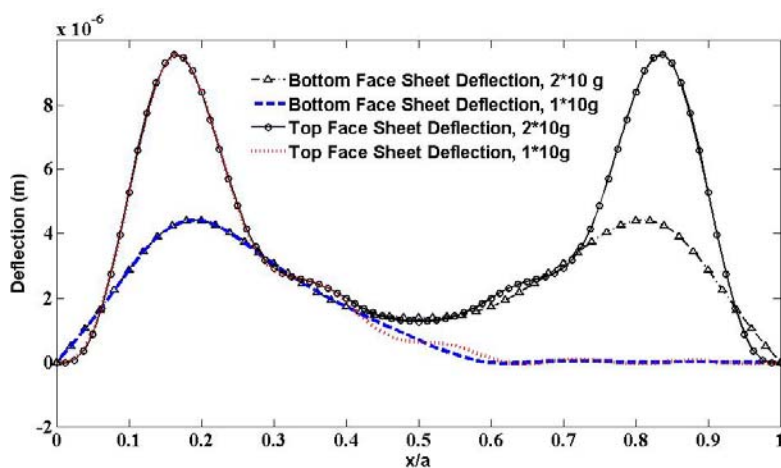


Fig. 8 Comparing maximum transverse deflections of two cases at the top and bottom face-sheets through the impact points on the top face-sheet along the section  $y = b/2$

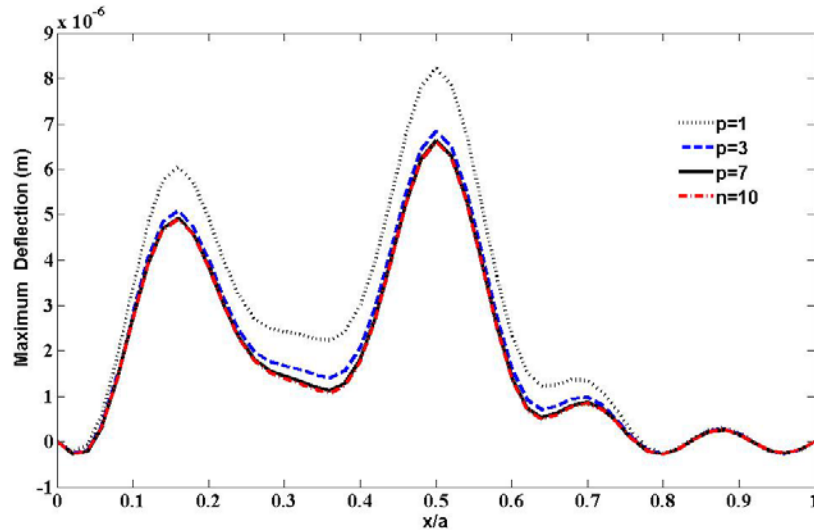


Fig. 9 Variation of maximum deflections of the top face-sheet with respect to increase of the power of FGM function of the core

Table 2 Properties of the sandwich panels with FG core

0 / 90 / 0 / FGM core / 0 / 90 / 0	Material properties
The top face sheet	$E_1 = 24.51 \text{ GPa}$ , $E_2 = 7.77 \text{ GPa}$ , $G_{12} = 3.34 \text{ GPa}$ , $G_{23} = G_{13} = 1.34 \text{ GPa}$ , $\rho = 1800 \text{ kg/m}^3$ , $\nu = 0.078$
The bottom face sheet	$E_1 = 24.51 \text{ GPa}$ , $E_2 = 7.77 \text{ GPa}$ , $G_{12} = 3.34 \text{ GPa}$ , $G_{23} = G_{13} = 1.34 \text{ GPa}$ , $\rho = 1800 \text{ kg/m}^3$ , $\nu = 0.078$
FGM-core	$E_1(x) = 80.4e6$ , $E_1(y) = 7.77 \text{ GPa}$ , $G_1(xy) = 32.2e6$ , $G_1(xz) = 120.6e6$ , $G_1(yz) = 75.8e6$ , $\rho_1 = 64 \text{ kg/m}^3$ , $\nu_1 = 0.3$ , $E_2(x) = 24.51 \text{ GPa}$ , $E_2(y) = 7.77 \text{ GPa}$ , $G_2(xy) = 3.34 \text{ GPa}$ , $G_2(yz) = G_2(xz) = 1.34 \text{ GPa}$ , $\rho_2 = 1800 \text{ kg/m}^3$ , $\nu_2 = 0.078$

approximately similar. Fig. 7 shows that the contact force histories of impacts with  $2 \times 10 \text{ g}$  mass impactors in locations  $(x_{1,2} = a/6, 5a/6, y_{1,2} = b/2)$  and  $1 \times 10 \text{ g}$  mass impactor in  $(x = a/6, y = b/2)$  were in good agreement. Maximum discrepancy between maximum contact forces and contact times obtained from spring mass and coupled complete models was 6.25% and 14.25%, respectively. Therefore, in order to calculate the contact force history of the small mass impact problem, analytical spring mass model was not suitable. In this example, maximum transverse deflections (complete solution method) of the top and bottom face-sheets along  $y$  direction are presented in Fig. 8. In order to show effect of power of FG functions and initial velocities of the impactors on dynamic behavior of sandwich panels, it was assumed that the impactors impacted in  $(x_1, y_1) = (a/6, b/2)$  and  $(x_2, y_2) = (a/2, b/2)$  on the top face sheet with mass of  $5 \text{ g}$  and velocities

of 3 and 4 m/s, respectively. In Fig. 9, variation of maximum deflections of the top face-sheet with respect to different cores with different powers of FGM function ( $p = 1, 3, 7, 10$ ) are shown. It can be seen from Fig. 9 that maximum deflections of the top face-sheets occurred under impact locations and also magnitudes of these parameters in location  $(x_1, y_1) = (a/2, b/2)$  were more than their magnitudes in other impact locations on the top face-sheet. This happened due to higher flexibility of the sandwich panel in location  $(x_1, y_1) = (a/2, b/2)$  and higher initial velocity of the impactor that was impacted in this location. Also, Fig. 9 shows that increase of the power of FGM function as core layer caused decrease of maximum deflections of the top face-sheet due to the increase of transverse stiffness of the sandwich panel.

### 3.2 Dynamic response of a sandwich panel with FG core subjected to multiple impactors and different masses at the same directions

This case occurs more in practical problems such as aerospace structures. In this case, it is important for the contact time of impactors not to be equal and for maximum deflection and other similar parameters not to be the same. In Tables 1 and 2, material properties of the face-sheets and the core are shown. Geometrical properties of the panel were ( $a = 158$  mm,  $a/b = 1$ ,  $a/h = 3.16$  and  $h_c/h = 0.88$ ). For example, a dynamic behavior of a sandwich panel subjected to two impactors with 10 g and 5 g masses and 3 m/s initial velocity, respectively, were investigated. Impacts occurred on panel in locations  $(x_1 = a/6, y_1 = b/2)$  with 5 g impactor mass and  $(x_2 = 5a/6, y_2 = b/2)$  with 10 g impactor mass. In Fig. 10, the three dimensional maximum deflection of the top face-sheet is shown.

In Table 3, for the sandwich panel with FG core, maximum impact forces in both impact locations ( $1 \times 5$  g at  $x = a/6$  and  $1 \times 10$  g at  $x = 5a/6$ ) are presented. It can be seen in Table 3 that impact force for foam core in both impact locations was usually smaller than the sandwich panel with arbitrary FG cores ( $P$ ,  $S$  and MT-FGM core). The difference of maximum impact force for arbitrary FG core was very low.

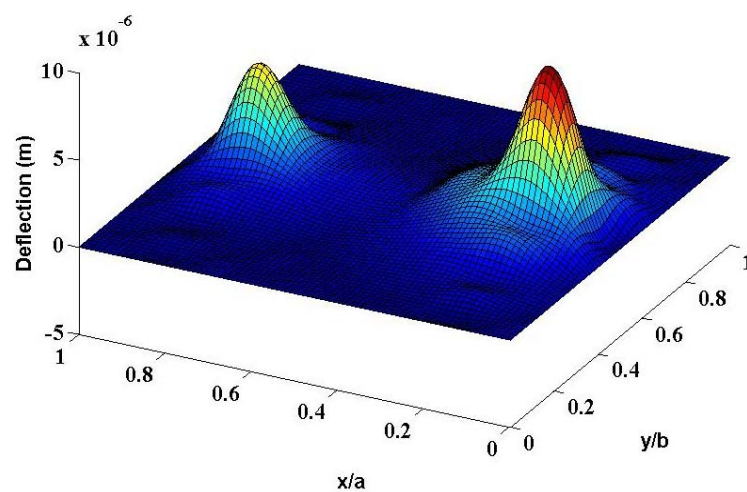


Fig. 10 Three dimensional view of the deflection of the top face-sheet

Table 3 Comparing maximum impact forces (N) for different types of the core

Type of the core	$1 \times 5$ gr at $(x, y) = (a/6, b/2)$	$1 \times 10$ gr at $(x, y) = (5a/6, b/2)$
Foam core	399.98	571.22
P-FGM core, $p = 1$	400.03	603.94
MT-FGM core, $p = 1$	399.83	603.13
E-FGM core	397.7	593.4
S-FGM core, $p = 1$	400.04	605.1

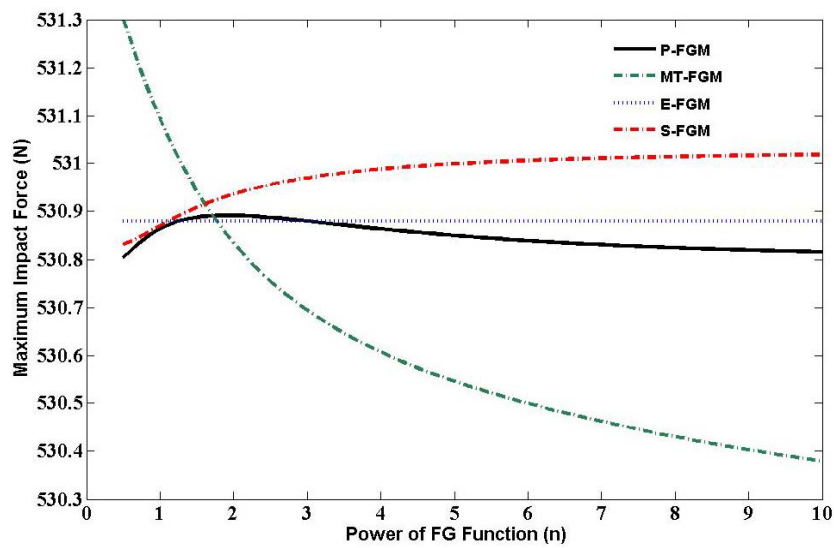


Fig. 11 Comparing maximum impact forces for the panels with different powers of FGM function

Fig. 11 shows variation of maximum impact force on the top face-sheet with power of FG core (P, E, S and MT-FGMs) in order to study effect of power of FG core function on maximum impact force. Fig. 11 shows that maximum impact force decreased with increasing power of FG function for MT-FGM cores and, for other FG cores, at first (until  $n = 1$ ), it increased and then reached constant values. Difference of maximum impact force at  $n < 1$  was more than  $n > 1$  due to different changes of properties of the cores through the core thickness.

### 3.3 Effect of the distance between the impactors on the dynamic behavior of the sandwich panels with FGM core

Another interesting case in sandwich panels subjected to multi impacts is effect of the distance between the impactors on dynamic behavior of the panel. Therefore, in order to show effect of this parameter, it was assumed that the sandwich panel was subjected to two impactors. Therefore, the impact locations  $(x_1/a, x_2/a) = (0.2, 0.5)$ ,  $(x_1/a, x_2/a) = (0.3, 0.5)$  and  $(x_1/a, x_2/a) = (0.4, 0.5)$  were considered. All the impacts occurred normally on the top face-sheets at  $y/b = 0.5$ . Properties

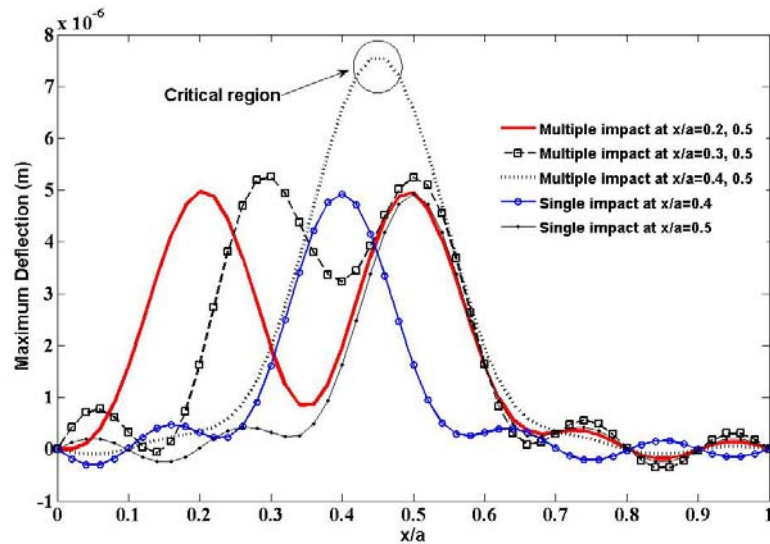


Fig. 12 Maximum transverse deflection of the top face-sheet with different distances between the impactors impacted on the top face-sheet

of the top and bottom face-sheets of the panel are given in Table 2 and core of the sandwich panel was P-FGM. The specimens incorporated a core with 44 mm thickness and overall dimensions of 158.7 mm  $\times$  and 158.7 mm ( $a/h = 10$ ,  $h_c/h = 0.88$ ). Mass of each impactor was 5 g, impact velocity of the impactors was 3 m/s and radius of the impactors was 5 mm. Maximum deflections of the top face-sheet for given impact locations are presented in Fig. 12. As can be seen in Fig. 12,

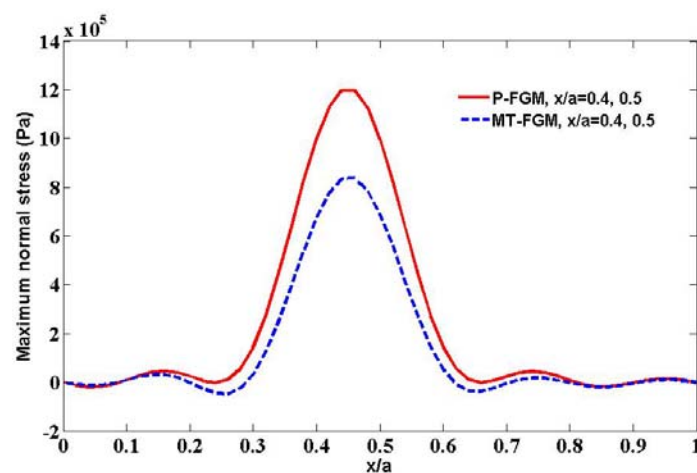


Fig. 13 Variation of maximum normal stresses in the top face-sheet of core interface of the sandwich panel subjected to two impactors in impact locations  $x/a = 0.4, 0.5$

when the first impact location changed from  $(x_1/a = 0.2)$  to  $(x_1/a = 0.3)$ , maximum deflections of the top face-sheet occurred under impact locations. Also, the region between the two impactors as deflected accordingly. But, when the first impact location reached  $x_1/a = 0.4-0.5$  or the distance between the two impactors reached  $0-0.1a$ , then the induced impact waves interacted between two impactors (see Eq. (36) of Ref. (Malekzadeh *et al.* (2006))) and maximum deflections of the top face-sheet occurred in the region between the two impactors. According to Eq. (36) of Ref. (Malekzadeh *et al.* (2006)), this region could be critical and it was very important in designing this case study and had to be considered in design process of the panel. Also, Fig. 12 shows that, in impact location  $(x_1/a, x_2/a) = (0.4, 0.5)$ , the results obtained from single impact at each of these locations and from multiple impacts were very different due to effect of the impactors on each other when distances were low. As can be seen in Fig. 12, the critical region was so important and could be dangerous in practical applications. So, studying normal and shear stresses in the critical region (i.e., the two impactors impacted on the top face-sheet in locations  $(x_1/a, x_2/a) = (0.4, 0.5)$ ) was important.

In this example, the two FG cores including  $P$  and MT FGM are considered as core layer of the sandwich panel and the results are compared. In Fig. 13 normal ( $\sigma_{zz}^c$ ) stresses for  $P$  and MT FG cores at the top interface ( $z = -hc/2$ ) are presented. As can be seen in Fig. 13, maximum normal stress for P-FGM ( $p = 1$ ) core was more than MT-FG core. Also, for both FGM cores, normal stress occurred in distance between two impact locations.

#### 4. Conclusions

In this paper, using the improved fully dynamic higher order sandwich panel theory, dynamic response of a sandwich panel with FG core under multiple impactors was studied. As seen from the results, the present model was in excellent agreement with alternative solutions and results of the experimental test for both single impact and multiple impacts. As seen in the results, because the impact force was assumed to be concentrated on the top face-sheet, gradient of deflections on impact region over top face-sheet was more than that on the bottom face-sheet and also the maximum deflections of top face-sheet were more than those on the bottom. This behavior occurred due to flexibility of the core. Also, increasing of the power of FGM function as the core caused decreasing of maximum deflections of the top and bottom face-sheet as well as maximum indentation which was due to the increase of transverse stiffness of the sandwich panel. The present method was capable of studying dynamic behavior of the sandwich panels under multiple impactors in opposite directions and different locations. According to Eq. (36) of Ref. (Malekzadeh *et al.* (2006)), the region between two impactors could be critical and it is very important in design process and must be considered. This region could be critical and it is very important in structural design problems.

#### References

- Abrate, S. (1998), *Impact on Composite Structures*, Cambridge University Press.  
 Anderson, T.A. (2005), "An investigation of SDOF models for large mass impact on sandwich composites", *Comp.: Part B*, **36**(2), 135-142.  
 Anderson, T.A. and Madenci, E. (2000), "Experimental investigation of low-velocity impact characteristics

- of sandwich composites”, *J. Comp. Struct.*, **50**(3), 239-247.
- Apetre, N.A., Sankar, B.V. and Venkataraman, S. (2002), “Indentation of a sandwich beam with functionally graded core”, *Proceedings of the 43rd AIAA Structures, Structural Dynamics and Materials Conference*, AIAA Paper no. 2002-1683, Denver, CO, USA.
- Bao, G. and Wang, L. (1995), “Multiple cracking in functionally graded ceramic/metal coatings”, *Int. J. Solids and Struct.*, **32**(19), 2853-2871.
- Bernard, M.L. and Lagace, P.A. (1989), “Impact resistance of composite sandwich plates”, *J. Reinf. Plastics and Comp.*, **8**(5), 432-445.
- Caprino, G. and Teti, R. (1994), “Impact and post-impact behavior of foam core sandwich structures”, *J. Comp. Struct.*, **29**(1), 47-55.
- Choi, I.H. and Hong, C.S. (1994), “New approach for simple prediction of impact force history on composite laminates”, *AIAA J.*, **32**(10), 2067-2072.
- Choi, I.H. and Lim, C.H. (2004), “Low-velocity impact analysis of composite laminates using linearized contact law”, *Comp. Struct.*, **66**(1-4), 125-132.
- Christoforou, A.P. and Swanson, S.R. (1991), “Analysis of impact response in composite plates”, *Int. J. Solid Struct.*, **27**(2), 161-170.
- Chung, Y.L. and Chi, S.H. (2001), “The residual stress of functionally graded materials”, *J. Chinese Inst. Civil Hydraulic Eng.*, **13**, 1-9.
- Dassault System’s Simulia Corp. (2008), *The ABAQUS 6.8-1 user’s manual*, USA.
- Delale, F. and Erdogan, F. (1983), “The crack problem for a non-homogeneous plane”, *ASME J. App. Mech.*, **50**(3), 609-614.
- Frostig, Y. (1998), “Buckling of sandwich plates with a flexible core: high-order theory”, *Int. J. Solids Struct.*, **35**(3-4), 183-204.
- Frostig, Y. and Baruch, M. (1994), “Free vibrations of sandwich beams with a transversely flexible core: A high order approach”, *J. Sound Vib.*, **176**(2), 195-208.
- Frostig, Y. and Thomsen, O.T. (2004), “High-order free vibration of sandwich panels with a flexible core”, *Int. J. Solids Struct.*, **41**(5-6), 1697-1724.
- Gong, S.W. and Lam, K.Y. (2000), “Effects of structural damping and stiffness on impact response of layered structures”, *AIAA J.*, **38**(9), 1730-1735.
- Gong, S.W., Lam, K.Y. and Reddy, J.N. (1999), “The elastic response of functionally graded cylindrical shells to low-velocity impact”, *Int. J. Impact Eng.*, **22**(4), 397-417.
- Hoo Fatt, M.S. and Park, K.S. (2001a), “Dynamic models for low-velocity impact damage of composite sandwich panels – Part A: Deformation”, *J. Comp. Struct.*, **52**(3-4), 335-351.
- Hoo Fatt, M.S. and Park, K.S. (2001b), “Dynamic models for low-velocity impact damage of composite sandwich panels – Part B: Damage initiation”, *J. Comp. Struct.*, **52**(3-4), 353-364.
- Khalili, M.R., Malekzadeh, K. and Mittal, R.K. (2005), “A new approach in static and dynamic analysis of composite plates with different boundary conditions”, *J. Compos. Struct.*, **69**(2), 149-155.
- Khalili, M.R., Malekzadeh, K. and Mittal, R.K. (2007), “Effect and physical and geometrical parameters on transverse low-velocity impact response of sandwich panels with a transversely flexible core”, *J. Comp. Struct.*, **77**(4), 430-443.
- Khalili, S.M.R., Soroush, M., Davar, A. and Rahmani, O. (2011), “Finite element modeling of low-velocity impact on laminated composite plates and cylindrical shells”, *Comp. Struct.*, **93**(5), 1363-1375.
- Kistler, L.S. and Waas, A.M. (1999), “On the response of curved laminated panels subjected to transverse impact loads”, *Int. J. Solids Struct.*, **36**(9), 1311-1327.
- Lal, K.M. (1983), “Residual strength assessment of low-velocity impact damage of graphite epoxy laminates”, *J. Reinf. Plast. Compos.*, **2**(4), 226-238.
- Malekzadeh, K., Khalili, M.R. and Mittal, R.K. (2005a), “Prediction of low-velocity impact response of composite sandwich panels using new three degrees-of-freedom model”, *The 13th International Conference of Mechanical Engineering*, Esfahan University of Technology, Esfahan, Iran, Paper code: 24.1418505.
- Malekzadeh, K., Khalili, M.R. and Mittal, R.K. (2005b), “Local and global damped vibrations of plates with

- a viscoelastic soft flexible core: An improved high-order approach”, *J. Sandwich Struct. Mat.*, **7**(5), 431-456.
- Malekzadeh, K., Khalili, M.R. and Mittal, R.K. (2007), “Response of composite sandwich panels with transversely flexible core to low-velocity transverse impact: A new dynamic model”, *Int. J. Impact Eng.*, **34**(3), 522-543.
- Malekzadeh, K., Khalili, M.R., Olsson, R. and Jafari, A. (2006), “Higher-order dynamic response of composite sandwich panels with flexible core under simultaneous low-velocity impacts of multiple small masses”, *Int. J. Solids Struct.*, **43**(22-23), 6667-6687.
- Mijia, Y. and Pizhong, Q. (2005), “Higher-order impact modeling of sandwich structures with flexible core”, *Int. J. Solids Struct.*, **42**(10), 5460-5490.
- Mittal, R.K. (1987), “A simplified analysis of the effects of transverse shear on the response of elastic plates to impact loading”, *Int. J. Solids Struct.*, **23**(8), 191-203.
- Olsson, R. (2000), “Mass criterion for wave controlled impact response of composite plates”, *Comp., Part A*, **31**(8), 879-887.
- Olsson, R. (2001), “Analytical prediction of large mass impact damage in composite laminates”, *J. Comp., Part A*, **32**(9), 1207-1215.
- Prakash, T., Singha, M.K. and Ganapathi, M. (2008), “Thermal post buckling analysis of FGM skew plates”, *Eng. Struct.*, **30**(1), 22-32.
- Reddy, J.N. (1997), *Mechanics of Laminated Composite Plates, Theory and Analysis*, CRC Press, FL, USA, Chapter 5.
- Reddy, J.N. (2003), *Mechanics of Laminated Composite Plates and Shells: Theory and Analysis*, CRC Press, FL, USA.
- Shivakumar, K.N., Elber, W. and Illg, W. (1984), “Prediction of low-velocity impact damage in composite laminates”, *AIAA J.*, **23**(5), 442-449.
- Sjoblom, P.O., Hartness, J.Y. and Cordell, T.M. (1988), “On low-velocity impact testing of composite materials”, *J. Compos. Mater.*, **22**(1), 30-50.
- Sokolinsky, V., Steven, R. and Frostig, Y. (2000), “Boundary condition effects in free vibrations of higher-order soft sandwich beams”, *AIAA J.*, **40**(6), 1220-1227.
- Sun, C.T. and Chattopadhyay, S. (1975), “Dynamic response of anisotropic laminated plates under initial stress to impact of a mass”, *J. Appl. Mech.*, **42**(3), 693-698.
- Sun, C.T. and Sankar, B.V. (1985), “Smooth indentation of an initially stressed orthotropic beam”, *Int. J. Solids Struct.*, **21**(2), 161-176.
- Swanson, S.R., Smith, N.L. and Qian, Y. (1991), “Analytical and experimental strain response in impact of composite cylinders”, *Compos. Struct.*, **18**(2), 95-108.
- Tarfaoui, M., Gning, P.B. and Hamitouche, L. (2008), “Dynamic response and damage modeling of glass/epoxy tubular structures: numerical investigation”, *Comp., Part A*, **39**(1), 1-12.
- Yang, S.H. and Sun, C.T. (1981), “Indentation law for composite laminates”, *Am. Soc. Test. Mater.*, ASTM STP 787, 425-449.
- Willis, J.R. (1966), “Hertzian contact of anisotropic bodies”, *J. Mech. Phys. Solids*, **14**(3), 163-176.

## Nomenclature

The following symbols are used in this paper:

$a, b$	Length and width of the sandwich panel, respectively.
$E_k^i$	Effective elastic modulus of the $i^{\text{th}}$ impactor ( $k = 1$ ) and target structure ( $k = 2$ )
$F_c^i(t), F^i(t)$	$i^{\text{th}}$ impact forces based on the linearized and Hertzian contact laws, respectively
$F_{c\max}^i$	Maximum impact force corresponding to the $i^{\text{th}}$ impactor
$h_t, h_b, h_c, h$	Thicknesses of the top and bottom face-sheets and core and panel, respectively.
$I_n^i$	Moments of inertia for the face-sheets and the core ( $n = 0, 1, 2$ ) ( $i = t, b, c$ )
$[K]$	Stiffness matrix of sandwich panel
$K_c^i, K_c^{*i}$	Contact stiffnesses of the Hertzian and linearized contact laws, respectively ( $i = 1, 2, \dots, N$ )
$K_g^i$	Stiffness of impacted face sheet at $i^{\text{th}}$ impact point
$k = \pi^2 / 12$	Shear correction factor
$M_I^i$	Mass of $i^{\text{th}}$ impactor
$M_{eff}^P$	Effective mass of the panel
$[M]$	Mass matrix of the sandwich panel
$M_z^c$	Normal bending moment per unit length of edge of the core
$M_{xy}, M_{xy}, M_{yy}$	Shear and bending moments per unit length of the edge
$n$	Exponent in the Hertzian contact law
$n_{xj}, n_{yj}$	In-plane shear loads along the longitudinal and transverse direction, respectively
$N_{xy}, N_{xx}, N_{yy}$	In-plane forces per unit length of the edge
$N^i$	Effective sandwich panel mass to the $i^{\text{th}}$ impactor's mass ratio
$N$	Numbers of impactors
$P$	Power of FGM functions
$q_j(x, y, t)$	Impact loads over the (top or/and bottom) impacted face-sheet ( $i = t, b$ )
$q_{mn}^i$	Fourier coefficients of the impact force distribution ( $i = 1, 2, \dots, N$ )
$Q_{xz}, Q_{yz}$	Shear forces in the face-sheets and core per unit edge length
$\{Q\}$	Vector of the impact forces
$R_z^c$	Normal force per unit length of edge of the core
$R^i$	Radius of the $i^{\text{th}}$ impactor
$T$	Kinetic energy
$t_2 - t_1$	Time interval of analysis
$t_{\max}^i$	Maximum contact time corresponding to the $i^{\text{th}}$ impactor
$u_k, v_k, w_k$	Unknowns of the in-plane displacements of the core

$u_c, v_c, w_c$	Displacement components of the core
$u_0^j, v_0^j, w_0^j$	Displacement components of the face-sheets ( $j = t, b$ )
$\ddot{u}_c, \ddot{v}_c, \ddot{w}_c$	Acceleration components of the core
$\ddot{u}_{0j}, \ddot{v}_{0j}, \ddot{w}_{0j}$	Acceleration components of the face-sheets ( $j = t, b$ )
$V^i$	Initial velocity of the $i^{\text{th}}$ impactor
$v_t, v_b, v_c$	Volumes of the upper and lower face sheets and core, respectively.
$z_t, z_b, z_c$	Normal coordinates in the mid-plane of the top and bottom face-sheets and core
$z_1^i(t), z_2^i(t)$	Deflections of the top face sheet and the $i^{\text{th}}$ impactor in the $i^{\text{th}}$ impact location
$\delta^i(t)$	Contact indentation for the $i^{\text{th}}$ impactor
$\delta_1^i$	Static displacement of impacted face sheet in the $i^{\text{th}}$ impact location
$\nu_k^i$	Effective Poisson's ratio of the $i^{\text{th}}$ impactor ( $k = 1$ ) and target structure ( $k = 2$ )
$\rho_t, \rho_b, \rho_c$	Material densities of the face-sheets and core
$\sigma_{ii}^i$	Normal stress in the face sheets ( $i = x, y$ ), $j = (t, b)$
$\sigma_{ii}^c$	Normal stress in the core ( $i = x, y, z$ )
$\tau_{xy}^c, \tau_{xz}^c, \tau_{yz}^c$	Shear stresses in the core
$\varepsilon_{0xx}^i, \varepsilon_{0xy}^i, \varepsilon_{0yy}^i$	Mid-plane strain components ( $i = t, b$ )
$\varepsilon_{zz}^c, \varepsilon_{xx}^c, \varepsilon_{yy}^c$	Normal strains components of the core
$\gamma_{xz}^c, \gamma_{yz}^c, \gamma_{xy}^c$	Shear strains components of the core
$\psi_x^j, \psi_y^j$	Rotation of the normal section of the face-sheet along y and x axes ( $j = t, b$ )
$\kappa_{xx}^i, \kappa_{yy}^i$	Curvatures in the x- and y-directions, respectively ( $i = t, b$ )
$\kappa_{xy}^i$	Torsion curvature of the face-sheets ( $i = t, b$ )